Available online at www.sciencedirect.com
SCIENCE DIRECT®
Journal of Structural Biology 145 (2004) 263–271
Journal of Structural Biology
www.elsevier.com/locate/yjsbi

Conformational and enzymatic changes of 20S proteasome of rat natural killer cells induced by mono- and divalent cations

Yana K. Reshetnyak,[1] Richard P. Kitson,[2] Min Lu,[3] and Ronald H. Goldfarb*,[2]

Department of Molecular Biology and Immunology, Institute for Cancer Research, University of North Texas Health Science Center, 3500 Camp Bowie Blvd., Fort Worth, TX 76107, USA

Received 21 July 2003, and in revised form 16 October 2003

Abstract

We have been investigated the relation between activation of ''neutral'' and ''acidic'' chymotrypsin-like (ChT-L) activity and conformational changes in the 20S proteasome complex from the rat natural killer (NK) cells induced by SDS, mono- and divalent cations. The conformational changes were monitored by tryptophan fluorescence and light scattering. It was revealed that the changes in the maximum position and contribution of the short-wavelength spectral component correlated with the alteration of ChT-L activity of the proteasome. Statistical analysis was applied to assign the fluorescence components with tryptophan residues based on the classification of calculated structural parameters of the environment of tryptophan fluorophores in protein. It was proposed that the emission of W13 from α6-subunit located near the cluster of highly conserved proteasome residues is mostly sensitive to the activation of the enzyme. We concluded that the expression of maximal ChT-L activity of 20S proteasome is associated with the conformational changes occurs in this cluster that lead to the proteasome open conformation, allowing substrate access into the proteolytic chamber.

Keywords: Proteasome; NK cell; Mono- and bivalent cations; Tryptophan fluorescence; Enzymatic activity; Structural analysis

1. Introduction

Nonlysosomal protein degradation is primarily mediated by the multicatalytic proteinase complex (MPC)[4] or proteasome, which is responsible for intracellular activities as diverse as the removal of misfolded proteins, cell cycle regulation via cyclin degradation, cellular immune responses by antigenic peptide processing (Baumeister et al., 1998; Ciechanover, 1994; Goldberg, 1995; King et al., 1996; Orlowski and Wilk, 2000; Rechsteiner et al., 2000). The 20S proteasome is a cylinder-shaped complex composed of four stacked rings consisting of 28 subunits. The outer rings are composed of seven α-subunits, and the inner rings of seven β-subunits, which contain the active sites responsible for at least three ''classical'' well-characterized proteolytic activities defined by their ability to cleave the peptide bonds after hydrophobic (chymotrypsin-like or ChT-L activity), basic (trypsin-like activity), and acidic (peptidylglutamyl-peptide hydrolyzing activity) amino acid residues (Orlowski and Wilk, 2000; Wilk and Orlowski, 1983). Mammalian 20S proteasomes have α- and β-subunits arranged in ordered unique ways and, upon induction by the interferon-γ, three β-subunits (LMP7, LMP2, MECL1) can replace three constitutively expressed subunits (X, Y, Z) leading to the molecular

* Corresponding author. Fax: 1-203-497-8533.
E-mail address: rgoldfarb@sopherion.com (R.H. Goldfarb).
[1] Present address: Department of Molecular Biophysics and Biochemistry, Yale University, 266 Whitney Avenue, P.O. Box 208114, New Haven, CT 06520-8114, USA.
[2] Present address: Sopherion Therapeutics, Inc., 300 George Street, New Haven, CT 06511, USA.
[3] Present address: Department of Pharmacology, The University of Texas Southwestern Medical Center, 5323 Harry Hines Blvd., Rm L5-100, Dallas, TX 75390-9042, USA.
[4] *Abbreviations used*: ChT-L, chymotrypsin-like; DTT, dithiothreitol; EDTA, ethylenedinitrilotetraacetic acid disodium salt; MPC, multicatalytic proteinase complex; NK, natural killer; SDS, sodium dodecyl sulfate; T-L, trypsin-like.

1047-8477/$ - see front matter © 2003 Elsevier Inc. All rights reserved.
doi:10.1016/j.jsb.2003.11.001

form reported as the "immunoproteasome" prevalently expressed in organs tissue involved in the immune response (Ortiz-Navarrete et al., 1991).

Some molecules are able to affect both the catalytic properties of the 20S proteasome or the mechanisms involved in the recognition of the substrate through the binding to specific sites on the catalytic subunits. It was reported that mono- and divalent ions, such as Na^+, K^+, Mg^{2+}, and Mn^{2+}, as well as SDS could change the proteolytic activity of MPC (Dahlmann et al., 1992; Djaballah and Rivett, 1992; Djaballah et al., 1993; Orlowski et al., 1991; Pereira et al., 1992; Saitoh et al., 1989; Wilk and Orlowski, 1983). In the present work we have investigated the relation between the activation or inhibition of the neutral and acidic chymotrypsin-like activity and conformational changes in the 20S proteasome complex from the rat natural killer (NK) cells induced by SDS, mono- and divalent cations. NK cells are large granular lymphocytes that lyse susceptible tumor cells, without apparent prior sensitization, in a major histocompatibility complex unrestricted manner (Trinchieri, 1989). Moreover NK cells are also potent mediators of antibody-dependent cell-mediated cytotoxicity (Titus et al., 1987). Numerous studies have been implicated the proteolytic enzymes as crucial to the cytolytic mechanism of these cells (Goldfarb, 1985; Hudig et al., 1993). A number of our studies indicated that a chymotryptic activity, which is a component of the 20S proteasome, contributed to the NK cell-mediated cytotoxicity (Goldfarb et al., 1992; Kitson et al., 2000; Wasserman et al., 1994).

2. Materials and methods

2.1. Materials

RPMI-1640 tissue culture medium, nonessential amino acids, antibiotics were purchased from Gibco (Grand Island, NY). Sucrose (Ultra-pure) was purchased from Beckman (Fullerton, CA). Ethylenedinitrilotetraacetic acid disodium salt (EDTA) was purchased from Fisher Scientific (Fair Lawn, NJ). Dithiothreitol (DTT), 2-mercaptoethanol, fluorogenic proteasome substrates: *N*-succinyl–Ala–Ala–Phe–7-amino-4-methylcoumarin (Suc–AAF–AMC), and *N*-succinyl–Leu–Leu–Val–Tyr–7-amino-4-methylcoumarin (Suc–LLVY–AMC); buffers: Hepes and Pipes were purchased from Sigma (St. Louis, MO). Amicon nitrogen pressure-based concentration apparatus and Diaflo 30 kDa cut-off filters were obtained from Amicon (Beverly, MA). Sephacryl S-400 heparin–Sepharose CL-6B chromatography media were purchased from Pharmacia (Piscataway, NJ). Glass columns were purchased from Kimble (Vineland, NJ) the fraction collection apparatus was purchased from ISCO (Lincoln, NE).

2.2. Cells

The CRNK-16 cell line was employed as a model for the NK cell function. CRNK-16 cells were maintained in RPMI-1640 containing 10% fetal bovine serum supplemented with L-glutamine, 1% (v/v) MEM nonessential amino acids, 5×10^{-5} M of 2-mercaptoethanol, and 100 U/ml penicillin and 100 μg/ml streptomycin antibiotics.

2.3. Protein preparation and purification

20S proteasome was purified from RNK16 cells following methods, which we have been described previously (Kitson et al., 2000; Wasserman et al., 1994). Briefly, subsequent to harvesting RNK16 cells, postnuclear supernatants were collected after nitrogen cavitation at 325–350 psi for 30–40 min. Successively, isopycnic sucrose gradient fractionation, Sephacryl S-400 gel filtration chromatography, and heparin–Sepharose CL-6B chromatography were applied. In each step, the protein concentration and the specific activities for proteasomal ChT-L and T-L activities were determined as previously described (Kitson et al., 2000; Wasserman et al., 1994).

2.4. Enzyme assays

MPC activity was measured by the monitoring of the fluorescence upon the cleavage of the fluorogenic synthetic peptides Suc–Leu–Leu–Val–Tyr–AMC and Suc–Ala–Ala–Phe–AMC. The Suc–Leu–Leu–Val–Tyr–AMC peptide was optimally cleaved at a neutral pH (buffer composition was 10 mM Tris–HCl and 1 mM EDTA, pH 7.5), while the Suc–Ala–Ala–Phe–AMC peptide is optimally cleaved at an acidic pH (buffer composition was 20 mM acetic acid and 1 mM EDTA, pH 5.5). The product formation was registered at 440 nm (excitation wavelength was 380 nm) during 5–7 min using a digital phase-modulation spectrofluorometer ISS K2 (ISS, Champagne, IL). The measurements were carried out at 25 °C. The slope of each curve was calculated using a linear least squares fitting. The correlation coefficient in each case was higher than 0.99.

2.5. Fluorescence and light scattering measurements

Tryptophan fluorescence and light scattering measurements were carried out on a digital phase-modulation spectrofluorometer ISSK2 (ISS, Champagne, IL) at 25 °C. The excitation wavelength was 295 nm, the emission spectra were recoded from 310 to 400 nm. The spectral widths of the excitation and emission slits were 4 and 2 nm, respectively. The polarizers in the excitation and emission paths were set at the "magic" angle (54.7° from the vertical orientation) and vertically (0°),

respectively, in order to reduce Wood's anomalies from the reflecting holographic grating. The emission spectrum of an aqueous solution of L-tryptophan was used as a standard for correction of protein spectra for the instrument spectral sensitivity (Burstein and Emelyanenko, 1996). The intensities of the corrected spectra were proportional to the number of photons emitted per unit wavelength interval. Decomposition of fluorescence protein spectra was performed according to the algorithms using program SIMS-MONO (Burstein et al., 2001; Reshetnyak and Burstein, 2001). The light scattering was measured at 400 nm wavelength settings of the excitation and emission monochromators.

2.6. Analysis of structural parameters of environment of tryptophan residues

Physical and structural parameters of the microenvironment of tryptophan residues from the crystal structure of bovine 20S proteasome (PDB entry 1IRU, (Unno et al., 2002)) was calculated using the algorithm for the analysis of the characteristics of environment of tryptophan residues in crystal structures of proteins in comparison with the fluorescence parameters of tryptophan fluorophores (Reshetnyak et al., 2001).

The set of structural parameters was obtained within the ranges of 0–5.5 and 5.5–7.5 Å from each atom of the indole rings of each of 38 tryptophan residues of MPC. Relative accessibility of indole fluorophore of tryptophan residue to water (Acc), the mean accessibility of Nε1 and Cζ2 atoms (Acc1-7) were calculated using a Lee and Richards algorithm (Lee and Richards, 1971) as the ratio (in per cent) of the accessible surface area of the atoms of indolic ring in protein and in free tryptophan residue in solution. Packing density (Den) is a number of neighbor atoms within the layer up to 7.5 Å around the indole ring. Parameter B was calculated as a mean value of the ratios of crystallographic temperature factors (Debye–Waller factor or B-factor) of all nitrogen, oxygen and sulphur atoms within the layers up to 5.5 and 7.5 Å around the indole ring to the mean B-factor value of all Cα atoms in crystal structure. To account for a common effect of both the mobility of neighbor polar atoms and the accessibility of the indole ring to free water molecules it was calculated parameter of dynamic accessibility (R): $R = \mathrm{Acc} \cdot B$. Parameter A was a mean value of the relative polarity of tryptophan environment in two surrounding layers (0–5.5 and 5.5–7.5 Å) (the details see in Reshetnyak et al., 2001).

Eventual quenchers of the tryptophan fluorescence were predicted based on the analysis of distances and orientations of potentially quenching groups (cystein SH and S–S groups, histidine imidazole or imidazolium, etc.) nearby the indole moiety (Burstein, 1976; Reshetnyak et al., 2001).

2.7. Calculation of probability of energy homo-transfer

The probability of excitation resonance energy homotransfer was estimated using a Förster equation (Lakowicz, 1999) with the parameters taken from Dale and Eisinger (1974) and orientation factors calculated from the mutual orientation of transition moments of the donors in ^1L_a state and the acceptors in either ^1L_a or ^1L_b states from atomic structure in cases when the centers of their indolic rings in proteins were separated by less than 12 Å.

2.8. Statistical analysis

For the classification of structural parameters of the tryptophan residues in MPC we used statistical method of cluster analysis (''STATISTICA for Windows 5.0'' StatSoft, 1984–1995). It was applied join or tree clustering algorithm and power distance (D) was used as a distance measure between objects (tryptophan residues):

$$D(x,y) = (\Sigma_i |x_i - y_i|^p)^{1/r}, \quad \text{where } p = 1,\ r = 4.$$

As an amalgamation rule we applied Ward's method that uses an analysis of variance approach to evaluate the distances between clusters (Ward, 1963).

Canonical analysis was employed for the calculation of root values for 38 tryptophan residues of MPC based on the classification of 137 tryptophan residues of 48 proteins obtained previously (Reshetnyak et al., 2001).

3. Results and discussion

3.1. Neutral and acidic chymotrypsin-like activities of 20S proteasome

We have been examined the relative effects of SDS, mono- and divalent cations on the ''neutral'' and ''acidic'' chymotrypsin-like activities of the 20S proteasome from the rat NK cells by measuring the rate of fluorescence increase during AMC formation (Table 1).

Table 1
The relative effect of mono- and divalent cations, and SDS on the degradation of Suc–LLVY–AMC (pH 7.5) and Suc–AAF–AMC (pH 5.5) by the 20S proteasome

Activator	Suc–LLVY–AMC, pH 7.5	Suc–AAF–AMC, pH 5.5
1 mM EDTA	100	100
0.035% SDS	213	15
5 mM Ca^{2+}	175	2
5 mM Mg^{2+}	163	3
0.1 mM Zn^{2+}	102	64
100 mM Na^{+}	39	28
100 mM K^{+}	41	27

Activities are expressed relative to the activities of the MPC toward each substrate in the absence of salts and SDS.

We used two different fluorogenic synthetic peptidic substrates: Suc–Leu–Leu–Val–Tyr–AMC and Suc–Ala–Ala–Phe–AMC, since it is known that the 20S proteasome is optimally active at neutral and acidic pHs against these substrates, respectively (Figueiredo-Pereira et al., 1995; Mason, 1990; Orlowski and Wilk, 2000). SDS, Ca^{2+}, and Mg^{2+} ions significantly stimulate the activity of the proteasome at pH 7.5, but completely inhibited it at pH 5.5. Divalent Zn^{2+} cation did not affect significantly the MPC activity at pH 7.5. However, the 20S proteasome expressed lower activity in the presence of Zn^{2+} ions in solution at the acidic pH. The effects of monovalent Na^+ and K^+ cations on the "neutral" and "acidic" ChT-L activities of the proteasome were very similar to each other. Both Na^+ and K^+ ions at the concentration of 100 mM decreased the rate of hydrolysis of fluorogenic substrate by 2-fold.

3.2. Structural changes in the 20S proteasome induced by mono- and bivalent cations

The conformational transitions in the 20S proteasome induced by SDS, mono- and divalent cations were studied by the steady-state fluorescence of tryptophan residues and light scattering (see Table 2). The area under the spectra (S) of the 20S proteasome was changed during various treatments. The most significant changes of the quantum yield were observed in the presence of SDS and divalent cations at both neutral and acidic pHs. The maximum position of the fluorescence spectra (335 ± 1 nm, calculated from the corrected fluorescence spectra) of the MPC was unchanged (data not shown). To perform the detailed study of the changes in the position and shape of fluorescence spectra we applied method of decomposition of tryptophan fluorescence spectra into log-normal components (Burstein et al., 2001). It was revealed that the best decomposition results were 2-component solutions in each case (see Table 2). The contributions of the spectral components (f) presented in Table 2 were recalculated to take into account the changes of the area under the spectrum. The tryptophan fluorescence spectra of the 20S proteasome at the neutral and acidic pHs decomposed into two spectral components are presented on the Fig. 1. The long-wavelength shift of the first spectral component and increasing of its contribution to the total spectrum indicated on the differences in conformational state of the MPC at pH 7.5 and 5.5.

At the neutral pH SDS, Mg^{2+}, and Ca^{2+} ions induced the decrease of the total intensity of fluorescence spectra for 12–16%, the long-wavelength shift of the first spectral component for ~5 nm (from 314.7 to 321.8 nm) and the increase of the contribution of this component for ~6%. This process was accompanied with the rise of the light scattering by about 2-fold without any changes in the anisotropy. The obtained data evidently indicate the conformational changes occurred in MPC in the presence of SDS, Mg^{2+} or Ca^{2+} cations, which are associated with the increase of the chymotryptic activity. Zn ions did not induce any conformational and enzymatic changes at the neutral pH. We did not observe any significant changes in the fluorescence and light scattering parameters of the MPC in the presence of monovalent cations, besides a slightly increased contribution of the short-wavelength spectral components. We concluded that the monovalent ions induced the

Table 2
Effect of mono- and divalent cations, and SDS on the area under the spectrum [S (%)]; maximum position of the spectral components [λ (nm)] and their contribution in total spectrum [f (%)] obtained as a result of fluorescence spectra decomposition; anisotropy (r) of tryptophan fluorescence and light scattering (L) of the 20S proteasome at pH 7.5 and 5.5

	pH 7.5				pH 5.5			
	S	$\lambda(f)$	r	L	S	$\lambda(f)$	r	L
1 mM EDTA	100	314.7 (15) 337.5 (85)	0.135	300	100	320.7 (24) 338.5 (76)	0.134	330
0.035% SDS	87	319.7 (23) 338.7 (77)	0.130	530	90	313.7 (21) 338.7 (79)	0.133	290
5 mM Ca^{2+}	88	320.3 (22) 338.7 (78)	0.138	610	134	309.6 (31) 338.8 (69)	0.191	>3000
5 mM Mg^{2+}	87	321.8 (21) 338.8 (79)	0.134	550	138	310.8 (28) 338.0 (72)	0.191	>3000
0.1 mM Zn^{2+}	101	315.3 (17) 337.8 (83)	0.132	320	112	312.1 (29) 339.2 (71)	0.134	350
100 mM Na^+	106	316.7 (25) 339.8 (75)	0.131	310	107	314.7 (26) 338.9 (74)	0.135	470
100 mM K^+	105	317.1 (26) 339.2 (74)	0.131	300	107	316.1 (24) 338.6 (76)	0.132	450

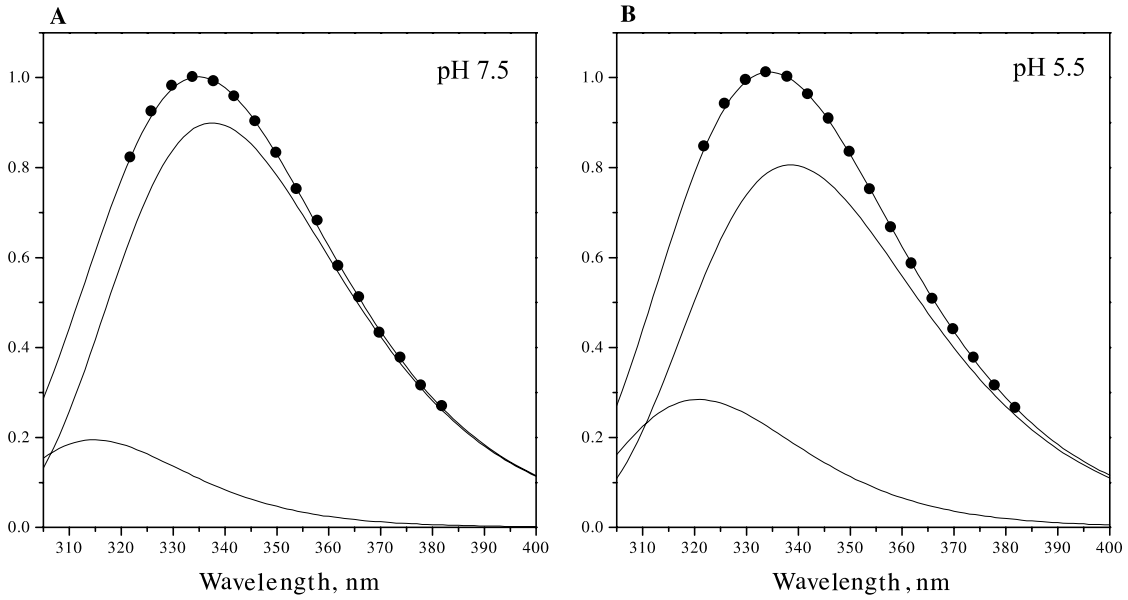

Fig. 1. Decomposition of normalized tryptophan fluorescence spectra of the 20S proteasome from NK cells in the presence of 1 mM EDTA into the log-normal components at pH 7.5 (A) and pH 5.5 (B) (experimental spectra—circles; fitting curves—lines). The maxima and relative contributions of the components are given in Table 2.

conformational changes in the proteasome. However, these changes were different from those induced by Mg^{2+} or Ca^{2+} cations. As a result the enzymatic activity decreased.

The most dramatic changes of the fluorescence parameters and light scattering of the 20S proteasome were monitored at the acidic pH in the presence of Mg^{2+} and Ca^{2+} ions. The increase of the anisotropy values (from 0.134 to 0.191), light scattering, the short-wavelength shift of the first spectral components with the increasing of its contribution in the total spectrum appears to suggest the aggregation process, which was accompanied by a complete loss of the enzymatic activity. While the acidic Ch-T activity of the 20S proteasome is considerably inhibited by the presence of SDS in solution, we observed rather opposite changes in the spectral parameters compared to that observed in the presence of divalent ions. This difference might be associated with different mechanisms of inhibition of the MPC enzymatic activity by SDS, magnesium or calcium ions at pH 5.5. The spectral changes of the tryptophan residues of the MPC induced by Zn^{2+} or monovalent ions were similar to each other. A slight shift towards the short wavelengths of the first spectral component was observed. However, the presence of monovalent ions lead to alterations in the light scattering values accompanied by the inhibition of enzymatic activity, which could be associated with changes of the proteasome size and/or shape. The obtained data are in a good agreement with sedimentation velocity and dynamic light scattering studies of MPC, which indicated that the activation and inhibition of the various proteolytic activities induced by mono- and divalent cations could be mediated by changes in size and shape of the molecule (Djaballah et al., 1993).

3.3. Analysis of the structural parameters of environment of tryptophan residues in the MPC

The analysis of fluorescence data revealed that the major spectral changes induced by mono- and divalent cations occurred with the first (short-wavelength) spectral component. To assign spectral components with tryptophan residues in the MPC we performed the detailed analysis of structural parameters of microenvironment of tryptophan fluorophores in crystal structure of the bovine 20S proteasome, which is a highly homological with the rat 20S proteasome. The 20S proteasome is a cylinder-shaped complex composed of two parts containing two stacked rings consisting of α- and β-subunits. There are 19 tryptophan residues located in each part of protein. Table 3 presents the numbers of tryptophan residues and their location in the subunits. The structural parameters of the microenvironment of tryptophan residues in the 20S proteasome were calculated using an algorithm described by Reshetnyak et al. (2001). The set of the structural parameters of 19 tryptophan residues (the averaged values of 38 tryptophan residues) of the MPC is presented in the first seven columns of Table 4. The calculated six parameters are: the accessibility of whole indole ring (Acc) and the mean accessibility of Nε1 and Cζ2 atoms (Acc1-7) of the tryptophan residue to water molecules; the packing density around the tryptophan (Den); the relative

Table 3
Numbers of tryptophan residues in crystal structure of the 20S proteasome and their location in the α- and β-subunits

Chains	Tryptophan residues
α-subunits	
α1	W101, W189
α2	W138, W157
α3	W139, W159
α4	W156
α5	W100
α6	W13
α7	W161, W215
β-subunits	
β1	W103
β2	—
β3	W154
β4	—
β5	W55, W104, W184
β6	—
β7	W91, W107, W209

mobility of the surrounding protein atoms (*B*); the relative mobility taking into consideration highly mobile water molecules (*R*); the parameter, which reflects the polarity of the environment around the tryptophan residue (*A*). Previously, based on the analysis of the spectral and structural properties of 137 tryptophan residues of 48 proteins it was demonstrated that these six structural parameters contribute into the canonical variate (root), which has the best correlation with the tryptophan fluorescence characteristics (Reshetnyak et al., 2001). The value of calculated canonical variate (root), which is a linear combination of six structural parameters, for 19 tryptophan residues of the MPC are presented in Table 4.

3.4. Assignment of tryptophan residues to spectral components

To classify the tryptophan residues of the proteasome based on the structural parameters we applied a method of cluster analysis. Fig. 2 demonstrates a hierarchical tree (dendrogram) constructed based on the canonical variate (root). The dendrogram revealed the clear "structure" and the existence of two distinct classes of the tryptophan residues (cluster A and B). Previously, it was estimated values of the canonical variate for the tryptophan residues, which belong to different spectral classes: Class A (emission at 308 nm)—root value was calculated as 3.6; Class S (322.5 ± 4.6 nm)—root = 3.2; Class I (331.0 ± 4.8 nm)—root = 1.2; Class II (342.3 ± 3.3 nm)—root = −0.8; Class III (347.0 ± 3.1 nm)—root = −6.6 (these data taken from (Reshetnyak et al., 2001)). The mean of the root values calculated for the tryptophan residues of the cluster A and B of the MPC were 1.64 and −0.85, respectively. Therefore, we can conclude that the tryptophan residues presented in the cluster A should emit at short wavelengths (320–328 nm), and fluorophores of the cluster B should contribute to the long-wavelength component with maximum at 338–343 nm. The positions of the spectral components predicted from the structural analysis (320–328 and 338–343 nm) are in a good correlation with the components obtained from the decomposition analysis of the fluorescence spectrum of the 20S proteasome

Table 4
Six structural parameters, canonical variate (root), which was calculated as a linear combination of six structural parameters, and classification of 19 tryptophan residues of the 20S proteasome

Trps	Acc	Acc1-7	Den	*B*	*R*	*A*	Root	Cluster
α-subunits								
W101, α1	8.4	0	129.5	1.009	8.5	33.6	1.68	A
W189, α1	5.5	1.8	119.0	0.967	5.3	35.3	1.26	A
W138, α2	23.7	39.6	99.0	1.016	24.1	53.2	−1.64	B
W157, α2	6.3	23.2	128.5	1.079	6.8	37.2	1.13	A
W139, α3	19.3	49.1	90.0	1.081	20.9	48.3	−2.06	B
W159, α3	12.2	30.7	106.0	0.972	11.9	47.1	−0.43	B
W156, α4	8.2	19.6	128.0	1.375	11.3	42.1	0.32	B
W100, α5	32.4	55.4	112.5	0.898	29.1	58.0	−1.41	B
W13, α6	0.8	0	145.5	0.902	0.70	40.5	2.83	A
W161, α7	13.6	33.6	99.0	1.251	17.0	48.4	−1.51	B
W215, α7	3.8	12.2	135.0	1.190	4.5	31.7	1.65	A
β-subunits								
W103, β1	9.4	25.0	97.0	1.070	10.1	45.9	−0.88	B
W154, β3	10.7	0	112.5	1.271	13.6	40.1	−0.30	B
W55, β5	5.4	5.4	122.0	0.831	4.5	27.5	1.88	A
W104, β5	12.0	35.1	101.0	1.221	14.7	48.0	−1.29	B
W184, β5	11.1	12.5	107.5	1.172	13.1	39.2	−0.24	B
W91, β7	13.3	53.6	106.0	0.786	10.5	32.5	0.01	B
W107, β7	18.8	63.7	103.0	0.773	14.2	42.2	−0.74	B
W209, β7	5.0	15.8	123.0	1.060	5.3	36.3	1.07	A

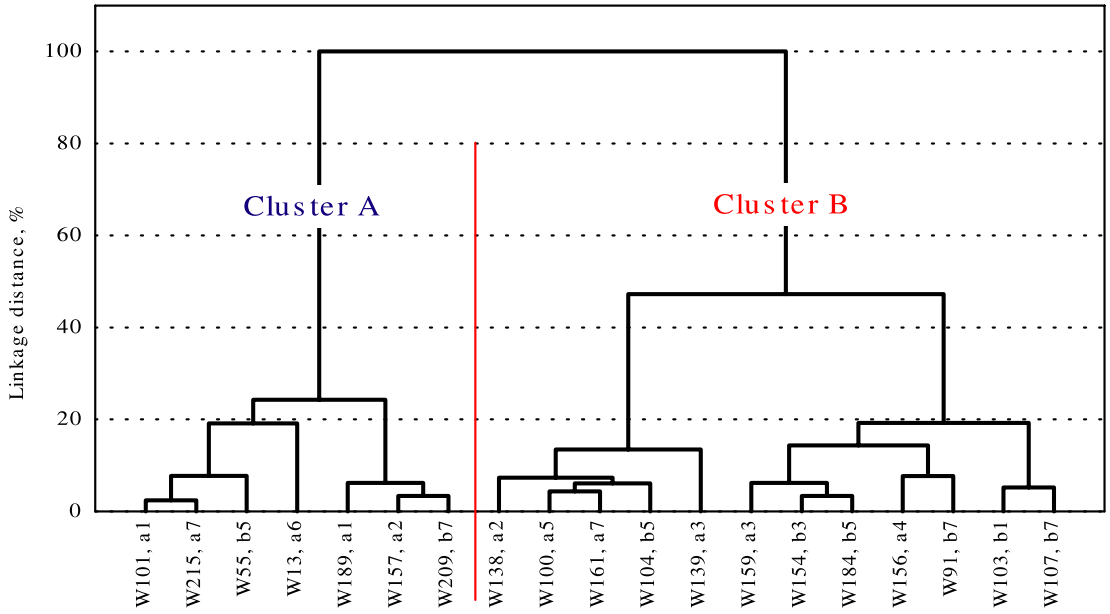

Fig. 2. Hierarchical tree (dendrogram) constructed based on the canonical variate (root).

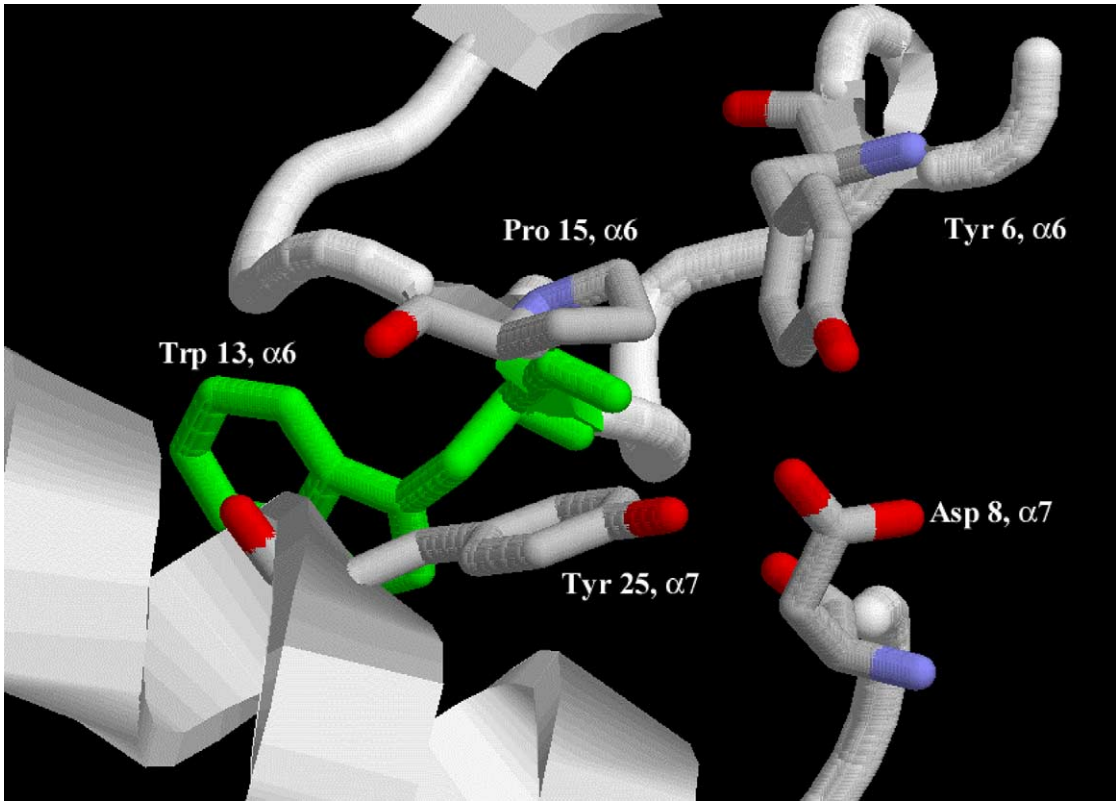

Fig. 3. Tryptophan residue W13, α6 is located near the cluster of highly conserved proteasome residues Tyr 6, α6; Asp 8, α7; Pro 15, α6; Tyr 25, α7.

measured in the presence of magnesium ions at pH 7.5 (~322 and 339 nm, see Table 2).

Fluorescence of the individual tryptophan residues might be partially or totally quenched by some protein groups (Bushueva et al., 1974, 1975; Chen and Barkley, 1998) or due to the resonance energy homo-transfer to other indole fluorophore(s) (Burstein, 1976; Konev, 1967). We analyzed the location and orientation of all possible quenching groups around the tryptophan residues. Also, we calculated the probability of resonance

Table 5
Tryptophan residues, which fluorescence might be partially or totally quenched due to the resonance energy homo-transfer or the interaction with nearly located protein-quenching groups

Tryptophan residues	Quenchers of tryptophan fluorescence (distance from Trp residue)
α-subunits	
W101 α1	Oη Tyr 107 α1 (3.6 Å); $N\varepsilon_2$ His 66 β2 (3.5 Å); Sδ Met 113 α1 (4.6 Å)
W138 α2	Sγ Cys 212 α2 (4.2 Å)
W157 α2	Nζ Lys 170 α2 (3.3 Å)
W156 α4	Sδ Met 59 α5 (5.1 Å)
W161 α7	Nζ Lys 182 α7 (4.1 Å); Sδ Met 181 α7 (4.6 Å)
W215 α7	Sγ Cys 186 α7 (4.9 Å)
β-subunits	
W154 β3	Sδ Met 14 β3 (3.6 Å); Sδ Met 158 β3 (4.5 Å)
W55 β5	Oη Tyr 90 β5 (3.8 Å); Sδ Met 86 β5 (3.7 Å); Sδ Met 97 β5 (5.2 Å)
W104 β5	24% of probability of energy transfer from Trp 104 β5 to Trp 184 β5
W91 β7	Sδ Met 70 β7 (3.7 Å)
W107 β7	Sδ Met 127 β7 (3.7 Å)
W209 β7	Oη Tyr 178 β7 (5.4 Å)

energy transfer between the indole rings of tryptophan fluorophores. Table 5 contains the list of tryptophans, which fluorescence could be partially or totally quenched.

At the next step we analyzed the structure of the cluster A, which was associated with the first spectral component (Fig. 2). This cluster contains 5 tryptophan residues from the α-subunits (W101, α1; W189, α1; W157, α2; W13, α6; W215, α7) and 2 tryptophan residues from the β-subunits (W55, β5; W209, β7). The contribution of tryptophan residues W101, α1; W157, α2; W215, α7; W55, β5; W209, β7 to the total emission of the MPC could be very low, since the quenching of tryptophan fluorescence by nearly located quenchers (see Table 5). Therefore, we can conclude that the tryptophan residues mostly contributing to the emission of the short-wavelength spectral component are located in the α-subunits of the 20S proteasome and they are W189, α1 and W13, α6.

3.5. Activation of the ChT-L activity of the MPC is associated with the conformational changes in a cluster of highly conserved proteasome residues of α-subunits

Activation of the proteasome might be achieved by different ways: interaction with 19S particle, γ-interferon-induced PA28 complex (11S activator regulator), mild chemical treatment, such as exposure to SDS and interaction with Mg and Ca ions. It was proposed that all these processes might be associated with some conformational changes in the N-terminal segments of the α-subunits, which lead to the opening of a channel into the core particle, allowing a substrate access into the proteolytic chamber (Groll and Huber, 2003; Groll et al., 1997, 2000). Particularly, it was demonstrated that interaction between four residues Tyr 6, Asp 8, Pro 15, Tyr 25, which pack against each other at the interface between each of the adjacent α-subunits stabilize open conformation and also are important for proteolysis by an archaeal proteasome (Förster et al., 2003; Whitby et al., 2000). These residues are invariant from archaea to human, including the species that appear to lack an 11S activator. Since W13, α6 is located at distance 4–9 Å from the cluster of residues Tyr 6, α6; Asp 8, α7; Pro 15, α6; Tyr 25, α7 (Fig. 3) we concluded that the emission of this tryptophan fluorophore is mostly sensitive to the activation of MPC that is associated with the conformational changes occurs in a cluster of four residues in the α-subunits. Particularly, the activation process (by SDS, Mg, and Ca ions at neutral pH) leads to the red-wavelength shift of the first spectral component, which could be result of the increasing mobility (disordering) of the cluster of four residues near W13, α6. We propose that the conformation of holo-form of the proteasome at acidic pH corresponds to the open conformation, since the spectral characteristics are very similar to those of the MPC in the presence of SDS, Ca or Mg ions at neutral pH, where the enzyme has the increased activity. The inhibition of the 20S proteasome activity is associated with enhance of fluorescence of the short-wavelength component without the significant spectral shift. It might be a result of stabilization of closed conformation of the MPC.

4. Conclusions

The obtained results indicate that the chymotrypsin-like activity of the 20S proteasome from NK cells could be modulated by SDS, mono- and divalent ions. The expression of maximal chymotrypsin-like activity, which contributes to the cytolytic mechanism of NK cells, is associated with the conformational changes occurs in a cluster of highly conserved proteasome residues from the α-subunits that lead to the proteasome open conformation, allowing substrate access into the proteolytic chamber.

Acknowledgments

The work was supported by a grant from the Robert A. Welch Foundation (BK-1396) to R.H.G.

References

Baumeister, W., Walz, J., Zuhl, F., Seemuller, E., 1998. The proteasome: paradigm of a self-compartmentalizing protease. Cell 92, 367–380.

Burstein, E.A., 1976. Adv. Sci. Technol. (Itogi Nauki i Tekhniki), ser. Biophysics, vol. 6, VINITI, Moscow, in Russian.

Burstein, E.A., Abornev, S.M., Reshetnyak, Y.K., 2001. Decomposition of protein tryptophan fluorescence spectra into log-normal components: I. Algorithm of decomposition. Biophys. J. 81, 1699–1709.

Burstein, E.A., Emelyanenko, V.I., 1996. Log-normal description of fluorescence spectra of organic fluorophores. Photochem. Photobiol. 64, 316–320.

Bushueva, T.L., Busel, E.P., Burstein, E.A., 1975. The interaction of protein functional groups with indole chromophore III. Amine, amide, thiol groups. Stud. Biophys. 52, 41–52.

Bushueva, T.L., Busel, E.P., Bushuev, V.N., Burstein, E.A., 1974. The interaction of protein functional groups with indole chromophore. I. Imidazole group. Stud. biophys. 44, 129–132.

Chen, Yu., Barkley, M.D., 1998. Toward understanding tryptophan fluorescence in proteins. Biochemistry 37, 9976–9982.

Ciechanover, A., 1994. The ubiquitin–proteasome proteolytic pathway. Cell 79, 13–21.

Dahlmann, B., Kuehn, L., Grziwa, A., Zwickl, P., Baumeister, W., 1992. Biochemical properties of the proteasome from *Thermoplasma acidophilum*. Eur. J. Biochem. 208, 789–797.

Dale, R.E., Eisinger, J., 1974. Intramolecular distances determined by energy transfer. Dependence on orientational freedom of donor acceptor. Biopolymers 13, 1573–1605.

Djaballah, H., Rivett, A.J., 1992. Peptidylglutamyl-peptide hydrolase activity of the multicatalytic proteinase complex: evidence for a new high-affinity site, analysis of cooperative kinetics, and the effect of manganese ions. Biochemistry 31, 4133–4141.

Djaballah, H., Rowe, A.J., Harding, S.E., Rivett, A.J., 1993. The multicatalytic proteinase complex (proteasome): structure and conformational changes associated with changes in proteolytic activity. Biochem. J. 292, 857–862.

Figueiredo-Pereira, M.E., Chen, W.E., Yuan, H.M., Wilk, S., 1995. A novel chymotrypsin-like component of the multicatalytic proteinase complex optimally active at acidic pH. Arch. Biochem. Biophys. 317, 69–78.

Förster, A., Whitby, F.G., Hill, Ch.P., 2003. The pore of activated 20S proteasomes has an ordered 7-fold symmetric conformation. EMBO 22, 4356–4364.

Goldberg, A.L., 1995. Functions of the proteasome: the lysis at the end of the tunnel. Science 268, 522–523.

Goldfarb, R.H., 1985. In: Herberman, R.B., Callewaert, D.M. (Eds.), Mechanisms of Cytotoxicity by NK Cells. Academic Press, New York, NY, pp. 205–212.

Goldfarb, R.H., Wasserman, K., Herberman, R.B., Kitson, R.P., 1992. Nongranular proteolytic enzymes of rat IL-2-activated natural killer cells. I. Subcellular localization functional role. J. Immunol. 149, 2061–2068.

Groll, M., Huber, R., 2003. Substrate access and processing by the 20S proteasome core particle. Int. J. Biochem. Cell Biol. 35, 606–616.

Groll, M., Bajorek, M., Kohler, A., Moroder, L., Rubin, D.M., Huber, R., Glickman, M.H., Finley, D., 2000. A gated channel into the proteasome core particle. Nat. Struct. Biol. 7, 999–1001.

Groll, M., Ditzel, L., Lowe, J., Stock, D., Bochtler, M., Bartunik, H.D., Huber, R., 1997. Structure of 20S proteasome from yeast at 2.4 Åresolution. Nature 386, 463–471.

Hudig, D., Allison, N.J., Ewoldt, G.R., Gault, R., Netski, D., Pickett, T.M., Redelman, D., Wang, M.T., Winkler, U., Zunino, S.J., Kam, C.-M., Odake, S., Power, J.C., 1993. In: Sitkovsky, M.V., Henkart, P.A. (Eds.), Cytotoxic Cells: Recognition, Effector Function, Generation, Methods. Birkhauser, Boston, MA, pp. 295–304.

King, R.W., Deshaies, R.J., Peters, J.-M., Kirschner, M.W., 1996. How proteolysis drives the cell cycle. Science 274, 1652–1659.

Kitson, R.P., Lu, M., Siman, R., Goldfarb, R.H., 2000. Proteasome inhibitor and lymphocyte function: partial inhibition of cell-mediated cytotoxicity and implication that the lymphocyte proteasome may contain multiple chymotryptic domains. In vivo 14, 265–268.

Konev, S.V., 1967. Fluorescence Phosphorescence of Proteins Nucleic Acids. Plenum Press, New York.

Lakowicz, J.R., 1999. Principles of Fluorescence Spectroscopy, second ed. Kluwer Academic/Plenum Publishers, NewYork.

Lee, B., Richards, F.M., 1971. The interpretation of protein structures: estimation of static accessibility. J. Mol. Biol. 55, 379–400.

Mason, R.W., 1990. Characterization of the active site of human multicatalytic proteinase. Biochem. J. 265, 479–484.

Orlowski, M., Wilk, S., 2000. Catalytic activities of the 20S proteasome, a multicatalytic proteinase complex. Arch. Biochem. Biophys. 383, 1–16.

Orlowski, M., Cardozo, Ch., Hidalgo, M.C., Michaud, C., 1991. Regulation of the peptidylglutamyl-peptide hydrolyzing activity of the pituitary multicatalytic proteinase complex. Biochemistry 30, 5999–6005.

Ortiz-Navarrete, V., Seelig, A., Gernold, M., Frentzel, S., Kloetzel, P.M., Hammerling, G.J., 1991. Subunit of the '20S' proteasome (multicatalytic proteinase) encoded by the major histocompatibility complex. Nature 353, 662–664.

Pereira, M., Yu, B., Wilk, S., 1992. Enzymatic changes of the bovine pituitary multicatalytic proteinase complex, induced by magnesium ions. Arch. Biochem. Biophys. 294, 1–8.

Rechsteiner, M., Realini, C., Ustrell, V., 2000. The proteasome activator 11 S REG (PA28) class I antigen presentation. Biochem. J. 345, 1–15.

Reshetnyak, Ya.K., Burstein, E.A., 2001. Decomposition of protein tryptophan fluorescence spectra into log-normal components: II. The statistical proof of discreteness of tryptophan classes in proteins. Biophys. J. 81, 1710–1734.

Reshetnyak, Ya.K., Koshevnik, Y., Burstein, E.A., 2001. Decomposition of protein tryptophan fluorescence spectra into log-normal components: III. Correlation between fluorescence microenvironment parameters of individual tryptophan residues. Biophys. J. 81, 1735–1758.

Saitoh, Y., Yokosawa, H., Shin-ichi, I., 1989. Sodium dodecyl sulfate-induced conformational and enzymatic changes of multicatalytic proteinase. Biochem. Biophys. Res. Commun. 162, 334–339.

Titus, J.A., Perez, P., Kaubisch, A., Garrido, M.A., Segal, D.M., 1987. Human K/natural killer cells targeted with hetero-cross-linked antibodies specifically lyse tumor cells in vitro prevent tumor growth in vivo. J. Immunol. 139, 3153–3158.

Trinchieri, G., 1989. Biology of natural killer cells. Adv. Immunol. 47, 187–376.

Unno, M., Mizushima, T., Morimoto, Y., Tomisugi, Y., Tanaka, K., Yasouka, N., Tsukihara, T., 2002. The structure of the mammalian 20S proteasome at 2.75 Å resolution. Structure 10, 609–618.

Ward, J.H., 1963. Hierarchical grouping to optimize an objective function. J. Am. Stat. Assoc. 58.

Wasserman, K., Kitson, R.P., Rivett, A.J., Sweeney, S.T., Gabauer, M.K., Herberman, R.B., Watkins, S.C., Goldfarb, R.H., 1994. Nongranular proteolytic enzymes of rat IL-2-activated natural killer cells. II. Purification identification of rat A-NKP 1 A-NKP 2 as constituents of the multicatalytic proteinase (proteasome) complex. J. Cell. Biochem. 55, 133–145.

Whitby, F.G., Masters, E.I., Kramer, L., Knowlton, J.R., Yao, Y., Wang, C.C., Hill, C.P., 2000. Structural basis for the activation of 20S proteasomes by 11S regulators. Nature 408, 115–120.

Wilk, S., Orlowski, M., 1983. Evidence that pituitary cation-sensitive neutral endopeptidase is a multicatalytic protease complex. J. Neurochem. 40, 842–849.